

## Efficient energy transfer in layered hybrid organic/inorganic nanocomposites: A dual function of semiconductor nanocrystals

Andrey A. Lutich,<sup>1,a)</sup> Andreas Pöschl,<sup>1</sup> Guoxin Jiang,<sup>1</sup> Fernando D. Stefani,<sup>1,b)</sup> Andrei S. Susha,<sup>2</sup> Andrey L. Rogach,<sup>2</sup> and Jochen Feldmann<sup>1</sup>

<sup>1</sup>*Department of Physics, Photonics and Optoelectronics Group, CeNS, Ludwig-Maximilians-Universität München, Amalienstrasse 54, 80799 Munich, Germany*

<sup>2</sup>*Department of Physics and Materials Science, City University of Hong Kong, Tat Chee Avenue, Kowloon, Hong Kong*

(Received 14 December 2009; accepted 23 January 2010; published online 24 February 2010)

The efficiency of energy transfer in hybrid organic/inorganic nanocomposites based on conjugated polymers and semiconductor nanocrystals is strongly dependent on both the energy transfer rate and the rate of the nonradiative recombination of the polymer. We demonstrate that the polymer nonradiative recombination can be reduced by the suppression of exciton diffusion via proper morphology engineering of a hybrid structure. In the layer-by-layer assembled nanocomposite of a conjugated polymer and CdTe nanocrystals the latter have a dual role: first, they are efficient exciton acceptors and, second, they reduce nonradiative recombination in the polymer by suppressing exciton diffusion across the layers. © 2010 American Institute of Physics. [doi:10.1063/1.3319838]

The development of hybrid organic/inorganic nanocomposite materials is a promising strategy to create new functional materials with tunable optical and electronic properties not accessible in any of the individual components. In particular, composites of conjugated polymers and semiconductor nanocrystals (NCs) have recently attracted significant attention because of their potential applications in light-emitting and photovoltaic devices.<sup>1,2</sup> In comparison to organic emitters, semiconductor NCs possess a number of advantages such as high photostability, broad spectral range of light absorption and narrow emission line widths.<sup>3</sup> On the other hand the conduction properties of closely packed NC films are poor,<sup>4</sup> making the electrical pumping of NCs inefficient. An evident approach to overcome this difficulty is designing a composite material where the NCs provide their advantageous luminescent properties and a conducting polymer provides efficient charge conduction.<sup>5</sup> Designing such nanocomposite materials requires a deep and detailed understanding of the energy transfer (ET) process from the organic to the inorganic component, which is still a subject of extensive research. Efficient ET has been reported<sup>6-9</sup> and the importance of the exciton diffusion has been verified<sup>10</sup> in the blended films of conjugated polymers and semiconductor NCs. Recently we've revealed that ET occurs rather via the Förster than the Dexter mechanism due to the nanoscale geometry of the system.<sup>11</sup> However, although a considerable understanding of the ET process has been achieved, the influence of morphology of such hybrid structures on the optoelectronic properties of the conjugated polymers and as a consequence on the ET process has not been understood and/or analyzed yet. In this work we explore by means of temperature dependent photoluminescence (PL) measurements the role of the morphology in the ET process in hybrid layer-by-layer (LbL) nanocomposites. We find that semicon-

ductor NCs have a dual function in LbL structures. First, they are very efficient energy acceptors and, second, they reduce nonradiative recombination of the polymer.

Following reported procedures we synthesized the water-soluble conjugated polymer poly[9,9-bis(3'-[(N,N-dimethyl)-N-ethylammonium]-propyl)-2,7-fluorene-alt-1,4-phenylene] dibromide [PDFD, Fig. 1(a)] (Ref. 11) with chain lengths of 10 to 20 repeat units and CdTe NCs capped with thioglycolic acid molecules [Fig. 1(b)]. On standard glass substrates we prepared hybrid nanocomposites consisting of 13 alternating layers of PDFD and CdTe NCs [Fig. 1(c)] using the LbL deposition technique based on the electrostatic interaction between oppositely charged polyelectrolytes and NCs.<sup>12</sup> We take advantage of the water solubility of positively charged PDFD to use it as a counterpart for negatively charged CdTe NCs in the LbL assembly. For reference, LbL assembled samples of CdTe NCs and PDFD with oppositely charged polyelectrolytes poly(diallyldimethylammonium chloride) (PDDA) and poly(sodium 4-styrenesulfonate) (PSS), respectively, were fabricated, where no ET between two materials takes place.

The total spectral overlap of the blue emission of PDFD and the absorption of CdTe NCs provides favorable conditions for the ET from PDFD to NCs, which is confirmed by the steady-state spectra shown in Figs. 1(d) and 1(e). The absorption and PL spectra of the PDFD/NC composite and the absorption spectrum of the PDDA/NC reference structure are shown in Fig. 1(d). The absorption band around 365 nm corresponds to PDFD. By comparing the absorption of the composite to the absorption of the components in solutions of known concentrations we estimate that approximately ten PDFD molecules per CdTe NC are present in the PDFD/NC composite. This corresponds to the 19% weight concentration of the NCs. The ET process is evident from the PL excitation (PLE) measurements [Fig. 1(e)] recorded at the peak emission wavelength of the NCs at 650 nm. For excitation wavelengths longer than ca. 450 nm only the NCs of PDFD/NC composite are excited and behave identically to the NCs in the PDDA/NC composite. As the excitation

<sup>a)</sup>Electronic mail: andrey.lutich@physik.uni-muenchen.de.

<sup>b)</sup>Present address: Departamento de Física, Facultad de Ciencias Exactas y Naturales, Universidad de Buenos Aires, Ciudad Universitaria, 1428 Buenos Aires, Argentina.

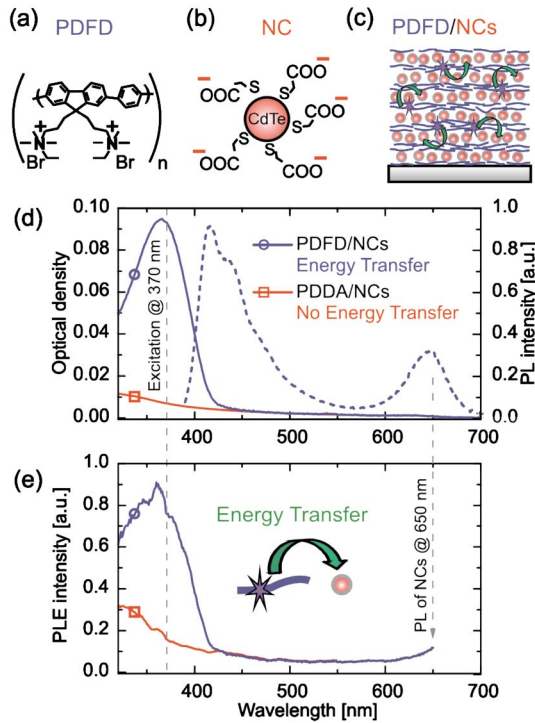


FIG. 1. (Color online) (a) Repeat unit of the poly[9,9-bis(3'-(N,N-dimethyl)-N-ethylammonium]-propyl)-2,7-fluorene-alt-1,4-phenylene] dibromide (PDFD). (b) Schematic representation of a CdTe NC capped with thioglycolic acid. (c) Schematic representation of a hybrid LbL PDFD/NC nanocomposite. (d) Steady-state absorption (solid lines) and PL (dashed line) spectra at the excitation wavelength of 370 nm. (e) PLE spectra at the emission wavelength of 650 nm. PDDA/NCs composite—squares, PDFD/NC composite—circles. The absorption and PLE spectra of the PDDA/NCs composite are normalized at the wavelength of 470 nm to the corresponding values of the PDFD/NC spectra.

wavelength is reduced below 450 nm, the PDFD molecules begin to absorb light and transfer energy to the NCs, which results in a higher PLE signal. At an excitation wavelength of 370 nm the PL intensity of the NCs is fivefold higher in the PDFD/NC structure as compared to the PDDA/NC structure.

Considering the increase of the PL intensity of NCs in the PDFD/NC composite the ET efficiency can be calculated using the following relation:<sup>13</sup>

$$\Phi_{ET} = \frac{A_{NC}^{PDFD/NC}(\lambda_{exc})}{A_{PDFD}^{PDFD/NC}(\lambda_{exc})} \left[ \frac{I_{NC}^{PDFD/NC}(\lambda_{exc})}{I_{NC}^{0,PDFD/NC}(\lambda_{exc})} - 1 \right], \quad (1)$$

where  $A_{NC}^{PDFD/NC}(\lambda_{exc})$  and  $A_{PDFD}^{PDFD/NC}(\lambda_{exc})$  are the absorbencies of the NCs and of the PDFD in the PDFD/NC composite, respectively, at the wavelength of excitation  $\lambda_{exc}$ .  $I_{NC}^{PDFD/NC}(\lambda_{exc})$  and  $I_{NC}^{0,PDFD/NC}(\lambda_{exc})$  are the integral PL intensities of the NCs in the PDFD/NC composite with and without ET, respectively. As a result we obtain  $\Phi_{ET} = 45\%$ .

For temperature dependent PL measurements the samples were mounted into a helium flow cryostat (Oxford Instruments) placed in the sample compartment of a Jobin-Yvon Fluorolog-3 spectrometer. Samples were excited through the glass substrate and PL was collected from the front face at an angle of 30°. PL spectra of the PDFD/NC composite sample were recorded consecutively at excitation wavelengths of 370 and 470 nm in the range of temperatures from 10 to 280 K. At an excitation wavelength of 370 nm ET from the PDFD to the NCs takes place. By probing the PL

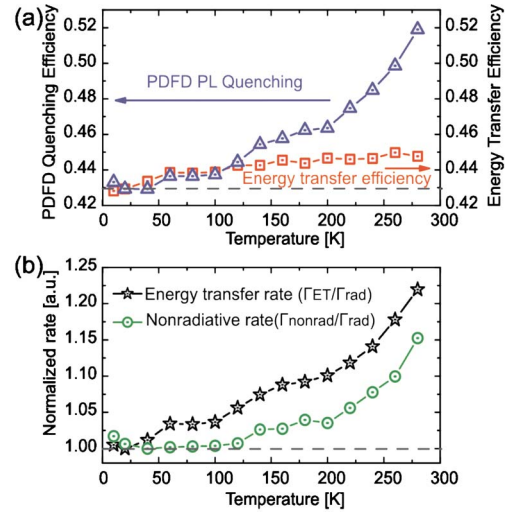


FIG. 2. (Color online) (a) Energy transfer efficiency (squares) and quenching efficiency of the PDFD (triangles) in the PDFD/NC composite vs temperature. (b) Ratios of the ET rate to the radiative rate (stars) and of the nonradiative rate to the radiative rate (circles) of the PDFD within the PDFD/NC composite as a function of temperature. The curves are normalized to unity at  $T = 20$  K.

intensity of the NCs the ET efficiency at different temperatures can be calculated using Eq. (1). PL spectra of the NCs at an excitation wavelength of 470 nm were measured to take into account the dependence of the quantum efficiency of NCs on temperature. We find that the ET efficiency in PDFD/NC composite is almost temperature independent: it only rises up from 43% to 45% upon increasing temperature from 10 to 280 K [Fig. 2(a)]. On the other hand, PDFD quenching efficiency increases from 43% to 52%. We define the quenching efficiency as  $\Phi_q = 1 - I_{PDFD}/I_{PDFD}^0$  and assume that at 20 K the ET is the only extrinsic process quenching PL of the PDFD (i.e.,  $\Phi_q = \Phi_{ET}$  at 20 K). The definitions of the ET efficiency [ $\Phi_{ET} = \Gamma_{ET}/(\Gamma_{rad} + \Gamma_{nonrad} + \Gamma_{ET})$ ] (Ref. 13) and the PL intensity of the PDFD [ $I_{PDFD} \propto \Gamma_{rad}/(\Gamma_{rad} + \Gamma_{nonrad} + \Gamma_{ET})$ ] within PDFD/NC composite can be rearranged as following:

$$\Gamma_{ET}/\Gamma_{rad} \propto \Phi_{ET}/I_{PDFD}, \quad (2)$$

$$(\Gamma_{nonrad}/\Gamma_{rad}) + 1 \propto (1 - \Phi_{ET})/I_{PDFD}, \quad (3)$$

where  $\Gamma_{rad}$  and  $\Gamma_{nonrad}$  are the radiative and nonradiative decay rates of the PDFD,  $\Gamma_{ET}$  is the ET rate from PDFD to NCs. Applying Eqs. (2) and (3) to the measured ET efficiencies and PDFD PL intensities at different temperatures and taking into account the PDFD quantum efficiency [ $1/(\Gamma_{nonrad}/\Gamma_{rad} + 1)$ ] of 9% at 20 K, the ratios of the rates  $\Gamma_{nonrad}/\Gamma_{rad}$  and  $\Gamma_{ET}/\Gamma_{rad}$  can be found [Fig. 2(b)]. The PDFD quantum efficiency was estimated by a comparison of the PL decay rates of the PDFD solid film at 20 K and PDFD in water solution with known quantum efficiency of 50%.

Assuming  $\Gamma_{rad}$  is independent of the temperature<sup>14</sup> we find that both  $\Gamma_{ET}$  and  $\Gamma_{nonrad}$  increase upon heating. It is known that thermally activated exciton migration in conjugated polymers effectively increases the ET rate from polymer to randomly distributed acceptor molecules.<sup>15</sup> On the other hand, the intrinsic (i.e., in the absence of NCs) quantum efficiency (IQE) of conjugated polymer films decreases with increasing temperature because of the growth of the

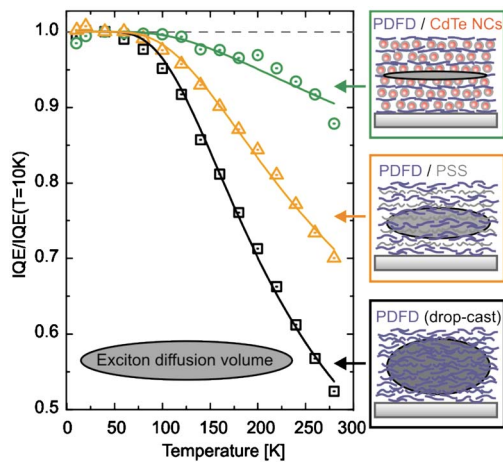


FIG. 3. (Color online) Intrinsic quantum efficiency vs temperature of the PDFD within nanocomposites with different morphologies: PDFD/NC LbL composite (circles), PDFD/PSS LbL composite (triangles), and bare PDFD layer (squares). The curves are normalized to unity at  $T=20$  K. The solid curves are results of an Arrhenius global data fit. The insets schematically illustrate corresponding nanostructures and volumes available for exciton diffusion (shaded regions).

nonradiative recombination rate. In order to use the full potential of hybrid nanocomposite structures, the ET efficiency from conjugated polymers to NCs has to be maximized by increasing the ET rate and suppressing nonradiative recombination in conjugated polymer.

In order to understand the physics underlying the observed temperature activated PDFD PL quenching and find a way to influence it we have studied the dependence of the IQE of PDFD on the morphology of the system. In addition to the measured temperature dependent IQE of PDFD within the PDFD/NC LbL nanocomposite, we have carried out temperature dependent PL measurements of PDFD within PDFD/PSS LbL composite and drop-casted bare PDFD films. We assume that in the absence of the energy acceptor (NCs) the IQE of PDFD is directly proportional to the measured PL intensity. The dependencies on temperature of the normalized IQE of PDFD in the three samples are shown in Fig. 3.

In all three cases the PDFD IQE is temperature independent up to roughly 100 K, and above that temperature it falls down rapidly. Such a behavior is characteristic of the thermally assisted motion of excitons in amorphous conjugated polymer films. From the Arrhenius global data fit we find activation energy of 40 meV of the exciton diffusion process. The decrease of IQE with temperature is clearly different for the samples having different morphologies, presenting an evident trend: temperature assisted IQE reduction is less efficient as the PDFD molecules are more separated from each other. This indicates that the main process responsible for the IQE reduction of the PDFD is exciton diffusion to quenching centers (defect polymer chains, impurities, etc.).<sup>16</sup> In the drop-casted PDFD layer an exciton may diffuse in all possible directions and, therefore, the probability of reaching a defect with following nonradiative recombination is relatively high. This leads to almost 50% IQE reduction upon increasing temperature from 10 to 280 K. In the PDFD/PSS LbL composite the layers of PDFD are separated by layers of PSS with an average thickness in the range of 0.5–1 nm.

Exciton diffusion across layers is therefore suppressed and consequently, the nonradiative recombination of excitons is reduced. As a result the IQE reduction at room-temperature is 30% in this case. Finally, in the PDFD/NC LbL composite the CdTe NCs impose a larger separation between PDFD layers because of their size of about 4 nm. This strongly hinders diffusion of excitons across the layers and reduces thermally assisted PL quenching down to only 10%.

In conclusion, we have shown experimentally that the energy transfer efficiency in hybrid organic/inorganic nanocomposites of conjugated polymers and semiconductor NCs is the result of the competition between the energy transfer process from the polymer to NCs and the nonradiative recombination in the polymer. The thermally activated exciton diffusion to quenching centers within the conjugated polymer layer is responsible for the increased nonradiative recombination rate. By proper morphology engineering of the hybrid structures the nonradiative recombination in conjugated polymers can be significantly reduced via suppression of exciton diffusion. In the LbL assembled nanocomposites the layers of semiconductor NCs play a twofold role, acting both as very efficient energy acceptors (energy transfer efficiency  $\sim 45\%$ ) and as insulating layers effectively suppressing nonradiative recombination in conjugated polymer layers via reduction of the exciton diffusion. The dual function of NCs in LbL composites makes these structures very attractive for applications in optoelectronics.

The authors acknowledge financial support of the DFG via the Project No. RO2345/5-1, the “Nanosystems Initiative Munich (NIM)” and the “LMUexcellent” program. A.A.L. and G.J. thank the Alexander von Humboldt foundation for financial support.

- <sup>1</sup>V. L. Colvin, M. C. Schlamp, and A. P. Alivisatos, *Nature (London)* **370**, 354 (1994).
- <sup>2</sup>W. U. Huynh, J. J. Dittmer, and A. P. Alivisatos, *Science* **295**, 2425 (2002).
- <sup>3</sup>A. L. Rogach, *Semiconductor Nanocrystal Quantum Dots* (Springer, New York, 2008).
- <sup>4</sup>C. A. Leatherdale, C. R. Kagan, N. Y. Morgan, S. A. Empedocles, M. A. Kastner, and M. G. Bawendi, *Phys. Rev. B* **62**, 2669 (2000).
- <sup>5</sup>S. Coe, W. K. Woo, M. Bawendi, and V. Bulovic, *Nature (London)* **420**, 800 (2002).
- <sup>6</sup>S. Kaufmann, T. Stöferle, N. Moll, R. F. Mahrt, U. Scherf, A. Tsami, D. V. Talapin, and C. B. Murray, *Appl. Phys. Lett.* **90**, 071108 (2007).
- <sup>7</sup>T. Chang, S. Musikhin, L. Bakueva, L. Levina, M. A. Hines, P. W. Cyr, and E. H. Sargent, *Appl. Phys. Lett.* **84**, 4295 (2004).
- <sup>8</sup>M. Anni, L. Manna, R. Cingolani, D. Valerini, A. Creti, and M. Lomascolo, *Appl. Phys. Lett.* **85**, 4169 (2004).
- <sup>9</sup>G. Jiang, A. S. Susha, A. A. Lutich, F. D. Stefani, J. Feldmann, and A. L. Rogach, *ACS Nano* **3**, 4127 (2009).
- <sup>10</sup>T. Stöferle, U. Scherf, and R. Mahrt, *Nano Lett.* **9**, 453 (2009).
- <sup>11</sup>A. A. Lutich, G. Jiang, A. S. Susha, A. L. Rogach, F. D. Stefani, and J. Feldmann, *Nano Lett.* **9**, 2636 (2009).
- <sup>12</sup>M. Y. Gao, C. Lesser, S. Kirstein, H. Möhwald, A. L. Rogach, and H. Weller, *J. Appl. Phys.* **87**, 2297 (2000).
- <sup>13</sup>B. Valeur, *Molecular Fluorescence: Principles and Applications* (Wiley, New York, 2002).
- <sup>14</sup>E. J. W. List, C. Creely, G. Leising, N. Schulte, A. D. Schlüter, U. Scherf, K. Müllen, and W. Graupner, *Chem. Phys. Lett.* **325**, 132 (2000).
- <sup>15</sup>B. P. Lyons and A. P. Monkman, *Phys. Rev. B* **71**, 235201 (2005).
- <sup>16</sup>M. S. Skolnick, D. M. Whittaker, T. A. Fisher, and P. E. Simmonds, *Phys. Rev. Lett.* **73**, 774 (1994).